A Big Data Analysis Approach for Rail Failure Risk Assessment

Ali Jamshidi*, Shahrzad Faghih-Roohi, Siamak Hajizadeh*, Alfredo Núñez*,**

Robert Babuska, Rolf Dollevoet*, Zili Li*, Bart De Schutter****

Abstract

Railway infrastructure monitoring is a vital task to ensure rail transportation safety. A rail failure could result in not only a considerable impact on train delays and maintenance costs, but also on safety of passengers. In this paper, the aim is to assess the risk of a rail failure by analysing the rail surface defects that are detected automatically among the huge amount of records from video cameras. We propose an image processing approach for automatic detection of rail defects, especially severe defects that are prone to rail breaks. We measure the visual length of the defects and use them to model the failure risk. For the assessment of the rail failure risk, we estimate the probability of rail failure based on the growth of defects. Moreover, we perform severity and crack growth analyses to consider the impact of rail traffic loads on defects in three growth scenarios. The failure risk estimations are provided for several samples of defects with different crack growth lengths on a busy rail track of the Dutch railway network. The results illustrate the practicality and efficiency of the proposed approach.

Keywords: Big data analysis, Rail surface defects, Rail failure risk, Image processing, Defect growth

1. INTRODUCTION

The railway network is one of the most successful transport systems for reducing transportation cost, traffic congestion, and air pollution emission levels. On the one hand, the increase in usage of the railway network requires a systematic monitoring plan to keep the trains running in a safe way as well as with the least possible disruptions.(1) On the other hand, a large amount of data is collected by frequent measurements from the monitoring systems of the infrastructure and the assets involved in the railway operations. This data should be controlled, stored, and processed, such that it can be employed to take all necessary actions to guarantee the rail asset quality level desired by the infrastructure manager.(2) The large amount of data should be processed into actionable knowledge within a certain time span.(3) In particular, the availability of data facilitates the prediction of the infrastructure health condition within a given time horizon. For this purpose, condition-based monitoring is typically proposed as a prognostic approach that brings consistent monitoring of the infrastructure health condition. It helps to keep the infrastructure manager continually informed of the estimated degradation of the railway infrastructure.(4) However, the database constructed from continuous monitoring of data will become larger and larger over time. Thus, applying a big data analysis approach is necessary in order to adequately monitor the infrastructure condition.(5,6)

Recent development in big data analytics for the operational risk analysis of industrial systems is studied by Choi et al.(7) Risk assessment of large-scale infrastructure systems is of current interest across many application domains.(8,9) Among all the railway infrastructure systems involved in the train operation, the rail track plays an important role in the railway networks. In an intensively used network, a considerable amount of the maintenance has to be allocated for the track, e.g., in the Dutch railway network, this amounts for almost half of the annual maintenance budget.[10] As a high percentage of failures occurring in the railway infrastructure are directly related to the rail, it is important to assess the failure risk of rails. More specifically, the rail risk assessment involves detecting the rail defects that can potentially result in rail break and derailment in extreme cases.[11-17]

Rail surface defects are caused by different factors such as fatigue due to large number of trains passing over rail components at especially welds, joints, and switches.[18] Early detection of surface defects is important to mitigate disastrous consequences of rail breaks. There are different methods to diagnose the condition of rail defects, including ultrasonic measurements,[19] eddy current testing,[20] and guided-wave based monitoring.[21] In general, these methods are not able to detect defects in an early stage of growth, i.e. not until the defects are severe. In particular, detection of defects at the late stage of growth imposes extra operation and maintenance costs due to the fact that the only solution is to replace the rail.

To address the limitations of the current measurement methods, the use of video cameras installed on trains has become popular.[22-24] The use of video cameras avoids the error-prone, costly, and time-consuming process of manual rail monitoring. Moreover, the videos taken from side cameras enable the infrastructure manager to capture the real condition of other track components such as fasteners, switches, and sleepers. Using video cameras, one can simply monitor whether the visible defects are at the early or late stage of growth. This means that the infrastructure manager has the opportunity to observe how the defect evolves over time in order to take actions at the right moment and to focus on the most urgent places for maintenance operations. This can lead to a significant reduction in the operation costs induced by the defects and it can prevent potential risks of rail breaks, reducing the risk of derailment. Due to the large amount and the high resolution of the videos taken over the rail, an automatic detection algorithm is required to process the huge amount of images from those videos.

In this paper, after proposing a big data analysis approach for the automatic detection of rail defects, a failure probability model is proposed. To estimate the parameters of the failure probability model, a Bayesian inference method[25] is used. A few studies have been carried out on the application of Bayesian methods in safety of railway infrastructures.[25-29] In particular, hierarchical Bayesian models have been employed to predict the evolution of the main quality indicators related to railway track geometry degradation, including the standard deviation of longitudinal level defects and the standard deviation of horizontal alignment defects.[25] The goal is to use the modeled indicators for planning track maintenance operations. An investigation on railway ballast failures has been carried out using Bayesian inference to analyze the uncertainty induced by measurement errors of vibrations in the ballast failure zones.[26] A nonparametric Bayesian approach with a Dirichlet Process Mixture Model has been used to facilitate reliability analysis in a railway system.[27] Moreover, a Bayesian network model has been applied to address human errors and track degradation in train accident consequences.[28,29] Furthermore, the Bayesian inference method has been employed extensively to assess model uncertainty and robustness for stochastic data behaviors.[30,31] Moreover, the Bayesian approach has been compared with the usual Maximum Likelihood Estimate (MLE) method.[32,33] Using MLE, the failure rate can be estimated by a single value that maximizes the likelihood function. Prior belief regarding the probable value of the failure rate is unknown in the estimation model using the MLE method. On the contrary, Bayesian inference considers failure rate as random variable where the estimation output is a probability density function, rather than a single point as proposed in the MLE method. Therefore, in this paper, we select the Bayesian inference methodology for the estimation of parameters in the rail failure probability function.

In this paper, by relying on the proposed failure probability function and the characteristics of defects detected by the proposed big data analysis approach, a failure risk model is constructed.

The main focus in the model is on analyzing the effects of rail surface defects. As a case study, a particular type of defects in railway networks called squats is considered. For this purpose, two main factors should be taken into account. The first factor is the stochasticity of the evolution of the defects. The second factor is the Million Gross Tons (MGT) due to which the rail structure deteriorates by the repeated passing of trains over rails. In this paper, a severity analysis approach is proposed to capture the visual length of defects as a function of MGT. Moreover, a crack growth analysis will be performed to estimate the growth of the crack length as a function of the MGT. The estimation results from the two analyses are used to assess the rail failure risk.

This paper is organized as follows. In Section 2, the proposed failure risk assessment model is presented including the model framework and the analysis approach. Section 3 addresses a real-life case study of the Dutch railway network. Section 4 presents the results and discussions. Finally, in Section 5, conclusions are presented.

2. FAILURE RISK ASSESSMENT MODEL

In this section, we propose a failure risk model by analysing the rail surface defects. Image, ultrasonic,(34) and eddy current testing(20) can all be used to detect the defects that can lead to rail break. In this paper, we rely on both ultrasonic detection method and video image. With ultrasonic measurement, we derive a general characteristic of crack growth. To analyze the crack growth data, a prediction model and a Bayesian inference method are used. With video image, we analyze the growth of the visual length of defects. To detect the defects in the images, a big data analysis approach is applied. Then, the visual length of the detected defects is measured to be used for the assessment of failure risk model. The approach can be employed for any type of rail defects.

2.1. Risk Assessment: The Proposed Framework

The proposed risk assessment framework is based on a big data analysis approach as shown in Fig. 1. In Step 1, a big data analysis approach is used to detect and classify the rail defects from a large amount of images taken over the rails. In Step 2, the visual length of the detected defects is measured. The visual length of a defect is an indication of its severity. We perform a severity analysis to assess the growth of the visual lengths of defects as a function of MGT, shown by F_S.

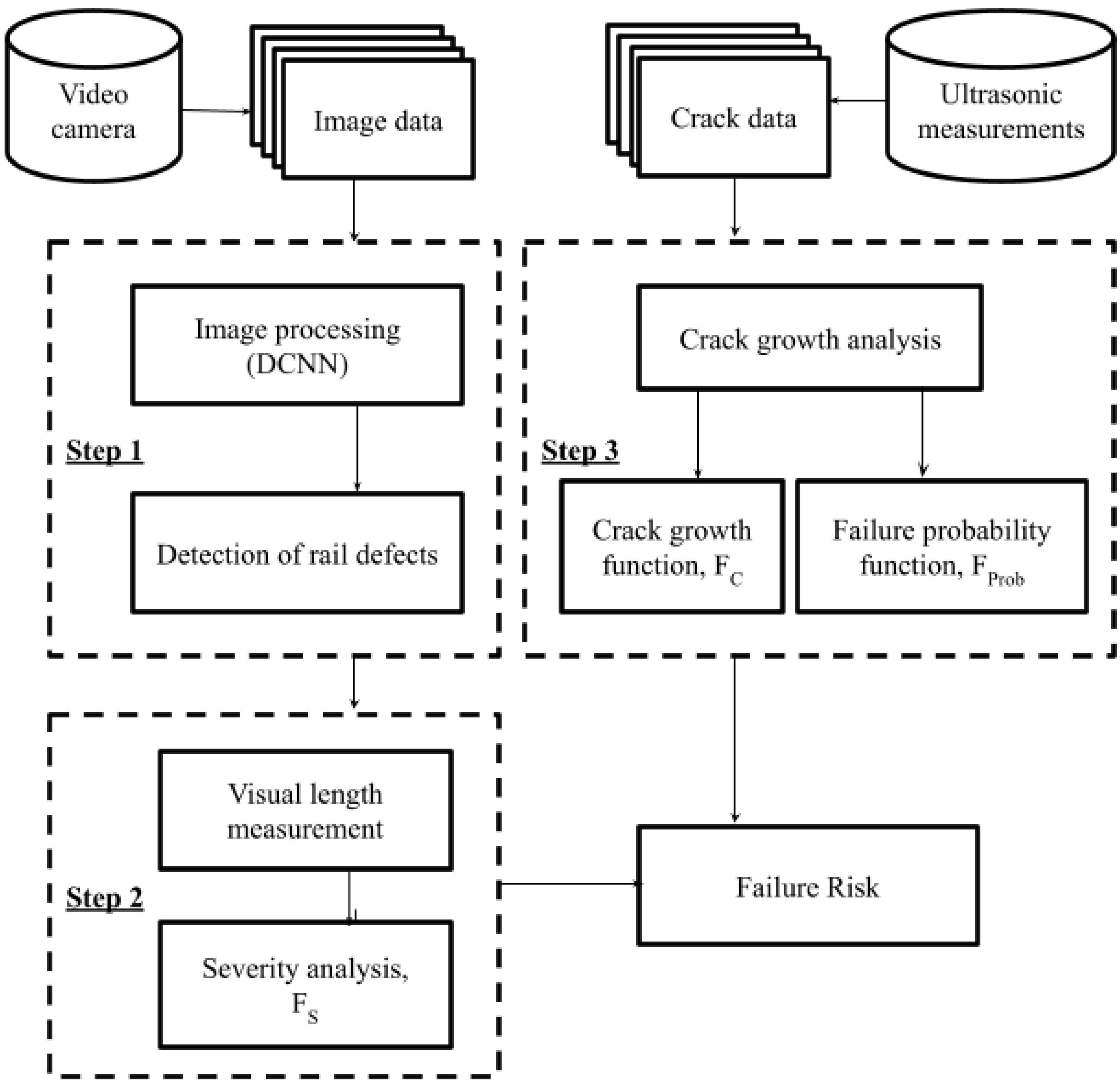

Fig. 1. Flowchart of the proposed methodology

In Step 3, a crack growth analysis is performed to estimate the crack growth as a function of MGT, F_C, using the data from ultrasonic measurements.[34] In addition, the probability of rail failure as a function of crack growth, F_{Prob}, is estimated using the crack growth data. Finally, we propose to assess the risk of rail failure with the composition of the probability function, the crack growth function, and the partially inversed of severity function:

$$\text{Risk} \propto F_{\text{Prob}}\left(F_C\left(F_{S,inv.}\left(V_1, V_2\right)\right)\right) \tag{1}$$

where V_1 and V_2 are two consecutive measurements of visual length for a defect, detected by analysis of image data, and $F_{S,inv.}$ relates V_1 and V_2 to MGT. Function F_C relates the estimate of MGT to crack growth, and function F_{Prob} estimates the probability of failure based on the estimate of crack growth. Thus, the risk is approximated relying on the failure probability achieved in (1). It means that the failure probability represents the risk of failure within a given MGT.

2.2. Analysis of Rail Image Data

We consider a railway health monitoring situation where a huge amount of video data is regularly collected. Subsequently, the video data needs to be analyzed in order to detect defects with a potential risk of rail break. The data is collected by a set of high frame rate cameras that are mounted on a measurement train. The video recordings cover the entire length of the measured distance on the rail track. The mounted cameras capture the rails from several angles to look at different components. The top view camera is aimed at the rail surface defects, with each frame covering a length of 15 cm of the track along the longitudinal direction. The recordings are preprocessed into video compilations where consecutive frames have a few millimeters of overlap and the effects of variations in the train speed are removed. As a result, recordings made from (bi)weekly measurements of roughly a thousand kilometer of rail amount to producing hundreds of Gigabytes. During the manual inspection process of the image recordings, only areas that are known to be extremely critical are inspected again by human experts, while most of the data is overwritten by the next measurement data simply to save disk capacity.

To be able to automatically extract defect information from the data, we train and apply a deep convolutional neural network (DCNN) to detect and classify the defects. Recently, application of DCNN has become very popular in the domain of big data due to the increases in the size of available training sets and algorithmic advances such as the use of piecewise linear units and dropout training.[35-37] By passing through a number of convolutional layers, the images are fed to the DCNN to train a set of shared neuron weights, referred to as filters. Convolution filters detect distinguishing features and form what is called a feature map. We use Rectified Linear Unit (ReLU)[38] activation functions after the convolution steps, and max-pooling layers to efficiently down-sample the outcome of each layer. Moreover, to prevent overfitting to the training data, we use dropout layers before each convolutional layer. Overfitting occurs when a classifier is fitted too closely to the sample data set that is unable to accurately describe the entire population, resulting into a high error over the test data. The dropout layer is known to prevent this by randomly disabling some activations from the previous layer.[39] The convolutional and pooling layer are finally attached to a sequence of three fully-connected layers to get class predictions.

The DCNN is trained by iterative feed forward of the training examples through the network, and by calculating the error with respect to the desired outcome. The error and its gradient are then evaluated at the last layer of the network and back-propagated through all the layers to adjust all the weights. Repeating this process until decreasing the error to a certain limit is called the gradient descent algorithm. [38] We use a widely applied variation of the algorithm where on each iteration, the error and gradients are calculated using a randomly selected set of training examples usually called a mini-batch.[38]

2.3. Severity Analysis

This section aims to model the visual length of defects based on the Million Gross Tons (MGT). MGT is a measurement unit to show the total weight of freight and passenger trains that pass over a given track in a given time horizon. Thus, the MGT can directly influence the growth of defects in the sense that an increase in the MGT accelerates the defect evolution process, and the tracks with a lower train occupation are expected to have a lower degradation rate than busy tracks.

The defects are automatically detected using the image processing method described in Section 2.2. We measure the visual lengths of the detected defects to use in severity analysis. We consider visual length as an indicator of a defect severity. Analysis of rail image data shows that the visual length of defects can grow with different rates as the MGT increases. Here, two ways of analysis can be considered to assess $F_{S,inv.}$ in (1):

Approach 1

Considering index m as an MGT increment counter, we propose an *N*-step ahead prediction model to describe the growth of visual length at different growth scenarios $h = h_1,\ h_2,\ \ldots,\ h_H$:

$$\begin{cases} \hat{V}_i^h(m+1) = F_S^h\left(\hat{V}_i^h(m), M^h(m)\right) & \textit{for } m = 0,1,\ldots,N-1 \\ \hat{V}_i^h(0) = V_i^h(0) \end{cases} \tag{2}$$

where $\hat{V}_i^h(m)$ is the estimate of the visual length for defect *i* at step m assuming scenario *h*, $M^h(m)$ as the total amount of MGT in step m, $F_S^h(\cdot)$ is the one-step ahead prediction function, and $V_i^h(0)$ is the visual length measurement at the current step.

By partially inversing $F_S^h(\cdot)$, we get $F_{S,inv.}^h$ as a function of the visual length in two consecutive MGT steps.

Approach 2:

In case of scarce data for the total amount of MGT in each step, an approximation can be made for the prediction model (2), considering a fixed value of m :

$$\hat{V}_i^h(m+1) = F_{S,approx.}^h\left(\hat{V}_i^h(m)\right) \tag{3}$$

We arrange a particular evolution for MGT and apply function $F_{S,approx.}^h$ in an *N*-step ahead fashion to reconstruct F_S^h . This yields to formulate the relation between visual length and MGT at step m. Once F_S^h is formulated, we can partially inverse it to get $F_{S,inv.}^h$ as follows:

$$MGT^h(m) = F^h_{S,inv.}\left(\hat{V}^h_i(m+1), \hat{V}^h_i(m)\right) \tag{4}$$

2.4. Crack Growth Analysis

2.4.1. Crack Growth With MGT

The crack growth of defects is an important factor in rail breaks. Independent of the defect severity, the growth of the crack length depends on the traffic load (MGT). The idea in this paper is to analyze the data measured by ultrasonic detection method[40], and to present a function for estimation of the crack growth over the MGT:

$$\Delta\hat{L}^h_i(m) = F^h_C\left(\hat{M}^h(m)\right) \qquad for\ m = 0,1,\ldots,N-1 \tag{5}$$

where $\Delta\hat{L}^h_i(m)$ is the estimate of the crack growth length for defect i at MGT step m assuming scenario h, and $F^h_C(\cdot)$ is the crack growth function. We will use a similar approach as described in Section 2.3 to assess the crack growth function.

2.4.2. Failure Probability

Regarding the crack growth data, assume the crack growth length, ΔL, contains I measures $(\Delta L_1, \Delta L_2, \ldots, \Delta L_I)$. The standard definition of a failure event is:

$$\bigcup_{i=1}^{I} \left\{\Delta L_i > d_i\right\} \tag{6}$$

where d_i is the critical level for the ith measurement. This formula implies that a failure occurs if the crack growth length exceeds the critical level. Logistic function is appropriate for these data since the response variable is binomial (failure if the measurement value satisfies (6), otherwise no failure).[41] Therefore, a logistic function is considered for the likelihood of rail failure probability $f\left(\Delta L|(a,b)\right)$ with parameters a (intercept) and b (slope).

Using a Bayesian inference model, variations of the model parameters can be considered as a step-wise degradation process. According to Bayes theorem, if prior knowledge about the parameters θ is represented by its probability density distribution $\pi_0\left(\theta\right)$, and if the statistical observations of crack growth length have likelihood $f\left(\Delta L\,|\,\theta\right)$, then rail failure probability can be expressed as posterior distribution π :

$$\pi\left(\theta|\Delta L\right)=\frac{f\left(\Delta L|\theta\right)\pi_0\left(\theta\right)}{f\left(\theta\right)}\propto f\left(\Delta L|\theta\right)\pi_0\left(\theta\right),\qquad \theta=(a,b) \tag{7}$$

Typically, Monte Carlo methods are used in Bayesian data analysis to derive the posterior distribution.[42,43] The aim of using a Monte Carlo method is to generate random samples from the posterior distribution in order to use them when it is impossible to analytically compute the posterior distribution. Among all the Monte Carlo methods, slice sampling is easier to implement as only the posterior needs to be specified.[44,45] The slice sampling algorithm selects samples uniformly from the region under the density function. Therefore, in this paper, a slice sampling algorithm is selected to capture the failure probability distribution.

[illegible] STUDY

[illegible]tion, the track Zwolle-Groningen from the Dutch railway network is considered to illustrate the capabilities of the proposed methodology. Track availability can be affected by rail surface defects. Among all types of rail surface defects, like rail corrugation, head checks, shatter cracking, vertical splits, head horizontal splits, and wheel burns, squats play an important role in having a significant impact on the health condition of the track. Therefore, our main focus is on detecting the squats in this case study.

In this case study, the track covers 105 km of rail starting from Zwolle to Groningen, corresponding to approximately 300,000 captured frames. The proposed DCNN architecture for analyzing this amount of image frames is presented in Fig. 2.

Initially the input images are down-scaled to 375×275 pixels and converted into gray-scale. The sequence of three fully-connected layers translates the extracted high-level features from the previous layers, into 3 classes representing the normal rail, trivial defects (seed squats), and squats.

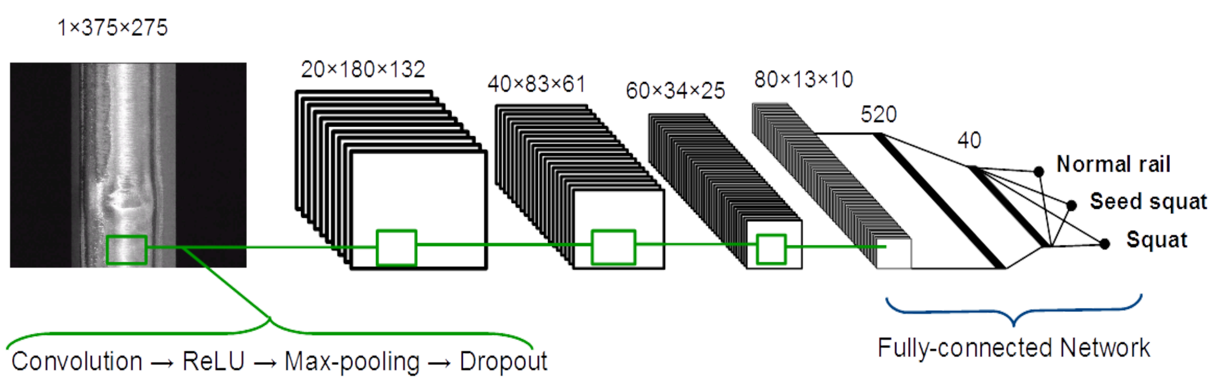

Fig. 2. Architecture of the proposed DCNN model

Trivial defects appear in the form of spots or small damages to the rail head, while squats are usually defects that are fully grown indentations and deformations of the rail surface. The normal class includes all other components such as plain rails, switches, welds, possible non-defect contaminations, etc. To train the network, a set of manually labeled examples is collected from several locations along the measured track and is compiled into a training set for each one of the 3 classes. Once the network is trained, it is used to find squats in the large pool of previously unseen samples. These samples are collected from other monitoring sessions. The average binary accuracy (squat vs. non-squat) of the network on all tested samples was equal to 96.9%. By putting a high acceptance threshold on the network output response, we opt to detect the correct cases of squats, trivial defects and the normal cases.

A sample of 109 detected squats of the track Zwolle-Groningen has been selected for measuring their visual lengths. Here, squats with a visual length below 15 mm are considered as light squats, in which cracks have not appeared yet (surface initiation is assumed, and from the image we cannot see beneath the surface). Squats with visual length ranging from 15 to 30 mm are considered to be at the medium stage of growth. The medium squats evolve to severe squats when the network of cracks spreads further.

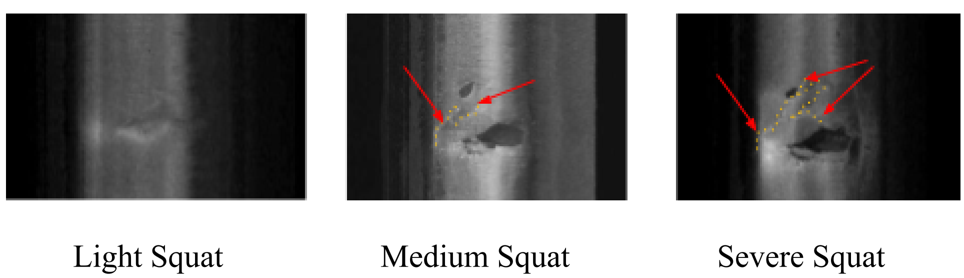

Fig. 3. A sample of squats in different classes of severity, the red arrows show the evolution of the crack when it gets severe.

Fig. 3 shows reference photos of squats ranging from light to severe together with crack evolution. After repeated train passages, light squats will evolve into medium or severe squats.[46]

Once the squat is severe, the squat will evolve into a defect with surface initiated cracks growing along the depth beneath the rail surface.[12]

After detecting squats by image processing , we apply Approach 2 as described in Section 2.2 for this particular case to construct severity function. From real data of visual length, we estimate $F^{h}_{S,approx.}$ from (3). Fig. 4 shows the relation between two consecutive measurements of visual length for a fixed value of MGT-step (m = 1). Relying on the physical understanding of how a squat grows, we fit a polynomial regression model of degree 3, using the least-absolute residual method[47], to represent the stochasticity of the growth. The residual plot together with the R-square value of 0.9778 determines how well the polynomial model fits the data. We consider the fit model as an average growth scenario, and the 3-sigma control limits as slow and fast scenarios.

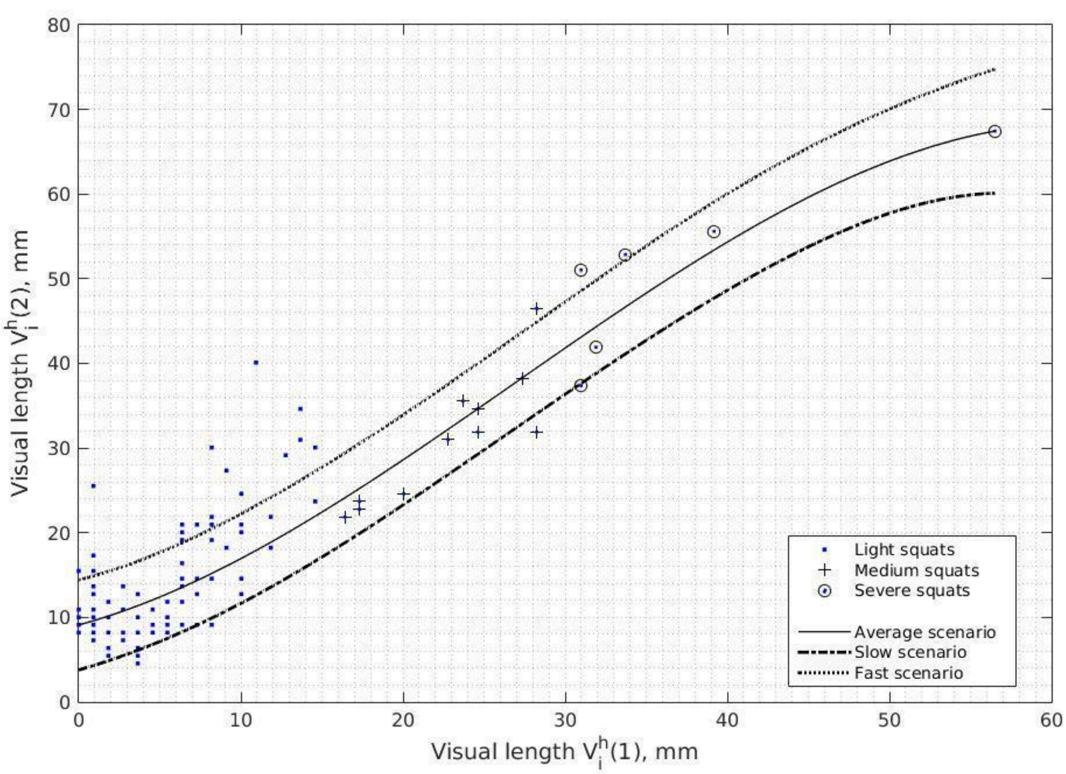

Fig. 4. Estimation of the visual length of the squats for m = 1, and based on real data

We use the estimated function of Fig. 4 for 8-step ahead prediction, and consider a fixed MGT increment of 3.01 in each step. As a result, a model-based prediction function for the visual lengths versus MGT is depicted in Fig. 5, considering the three scenarios of average (a), fast (b), and slow (c). The dotted line shows the upper bound of the estimation for visual length, i.e. it is very rare to observe a squat with a length over the upper bound in reality.

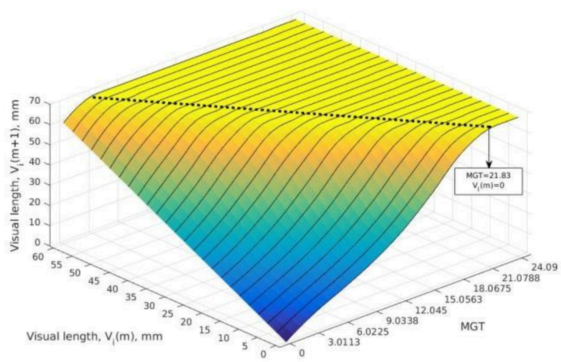

(a)

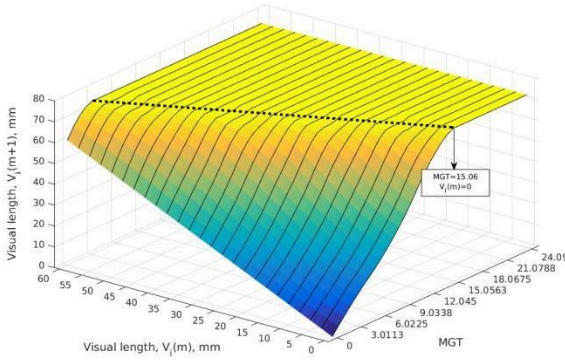

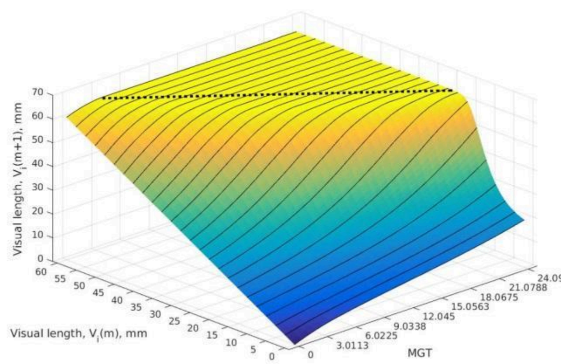

(b) (c)

Fig. 5. Growth of squat visual length over MGT for the following model-based growth scenarios: (a) average, (b) fast, (c) slow, the dotted line depicts an upper bound of squat visual length.

Assuming $V_i^h(m) = 0$, the visual length at MGT step $m+1$ at the fast scenario, reaches the upper bound with a MGT $(\mathrm{MGT}_{h_1} = 15.06)$, lower than at the average scenario $(\mathrm{MGT}_{h_3} = 21.83)$ and at the slow scenario $(\mathrm{MGT}_{h_2} = 51.32)$. It means that the degradation process at the fast scenario is more accelerated than at the average and slow scenarios as the traffic load on rail increases.

As described in Section 2.4.1, we estimate the crack growth function, $F_C^h(\cdot)$ by relying on ultrasonic measurement data. The model-based relation between the crack growth length and MGT is shown in Fig. 6. In addition, three different scenarios are considered to capture the crack growth dynamics, including the average scenario, the slow scenario, and the fast scenario.

As seen in the figure, at the fast scenario, crack propagation of the squat at a given MGT is significantly faster than squats that are at the average and the slow scenario. For example, at MGT = 10.36, it is estimated that the crack length of a squat grows 1 mm at the slow scenario, 2 mm at the average scenario, and 8 mm at the fast scenario. We can assess the risk of rail failure considering any of the different scenarios of crack growth length.

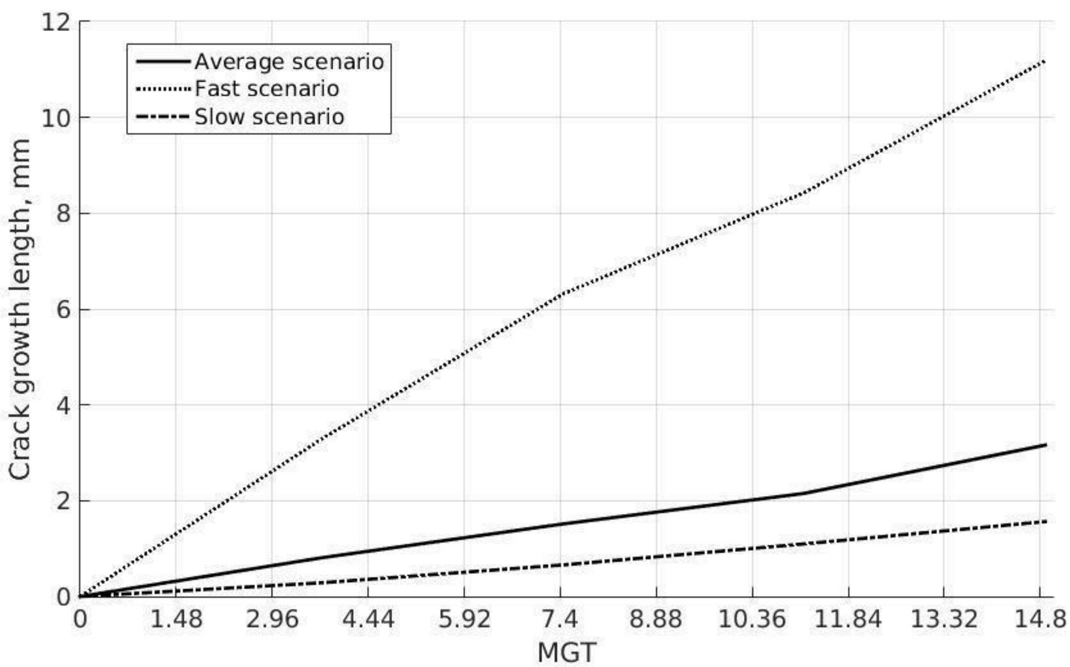

Fig. 6. A model-based relation between crack growth length and MGT

In the failure probability model, we consider that a rail is prone to fail when a squat reaches a crack length of 9 mm. The crack length of each squat is measured to see how it has grown over MGT, and how many cracks have reached a length of 9 mm or even more. We use normal priors for the regression parameters (a, b). Relying on the data for the crack growth length, the parameters are estimated by a slice sampling algorithm considering 1000 samples. Respectively, Fig. 7 and Fig. 8 shows how the mean of the parameter *a* and *b* varies over the samples and converges to a constant value. As seen in the figures, the posterior means of parameters converge to a stationary status after the first 50 samples.

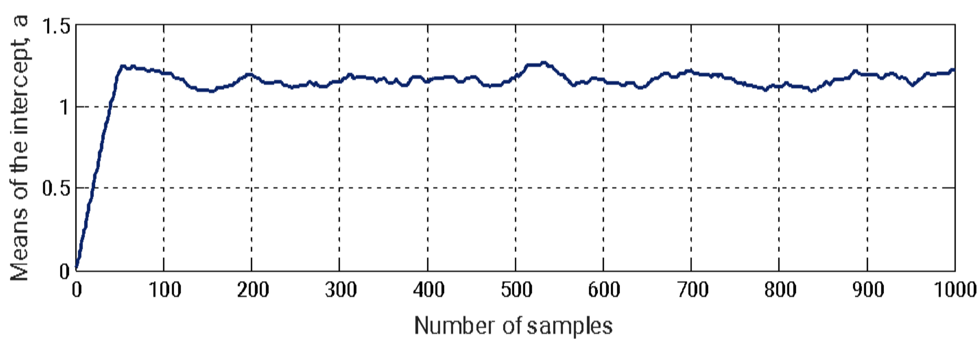

Fig. 7. Posterior distributions of regression parameter *a*

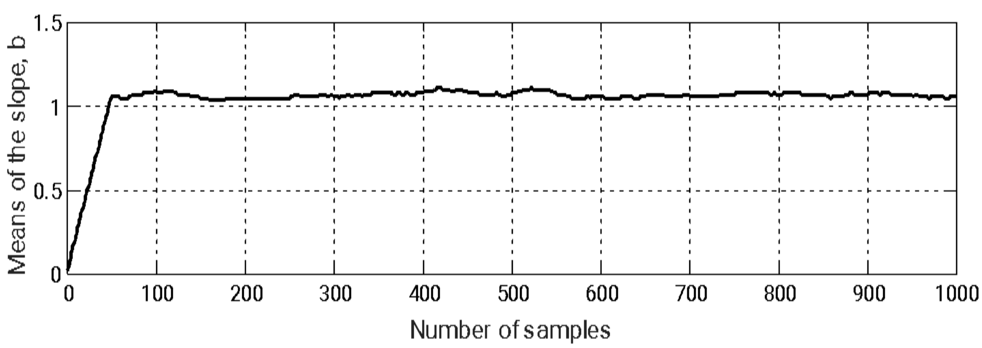

Fig. 8. Posterior distributions of regression parameter *b*

4. RESULTS AND DISCUSSION

For a detected squat with measured visual lengths in one MGT step, we estimate the risk of rail failure as follows: From the model in Fig. 5, we estimate the MGT for the visual lengths in two consecutive measurements. Then, from the model in Fig. 6, we find the crack growth length for the estimated MGT. Finally, we estimate the failure probability from the crack growth length in Fig. 9.

The failure probability plot represents how probable a squat fails in the next MGT step when the crack growth length is given. As an example, if the crack length of a squat increases 6 mm for MGT =7.04, the probability that the squat could lead to a rail break is roughly 0.82.

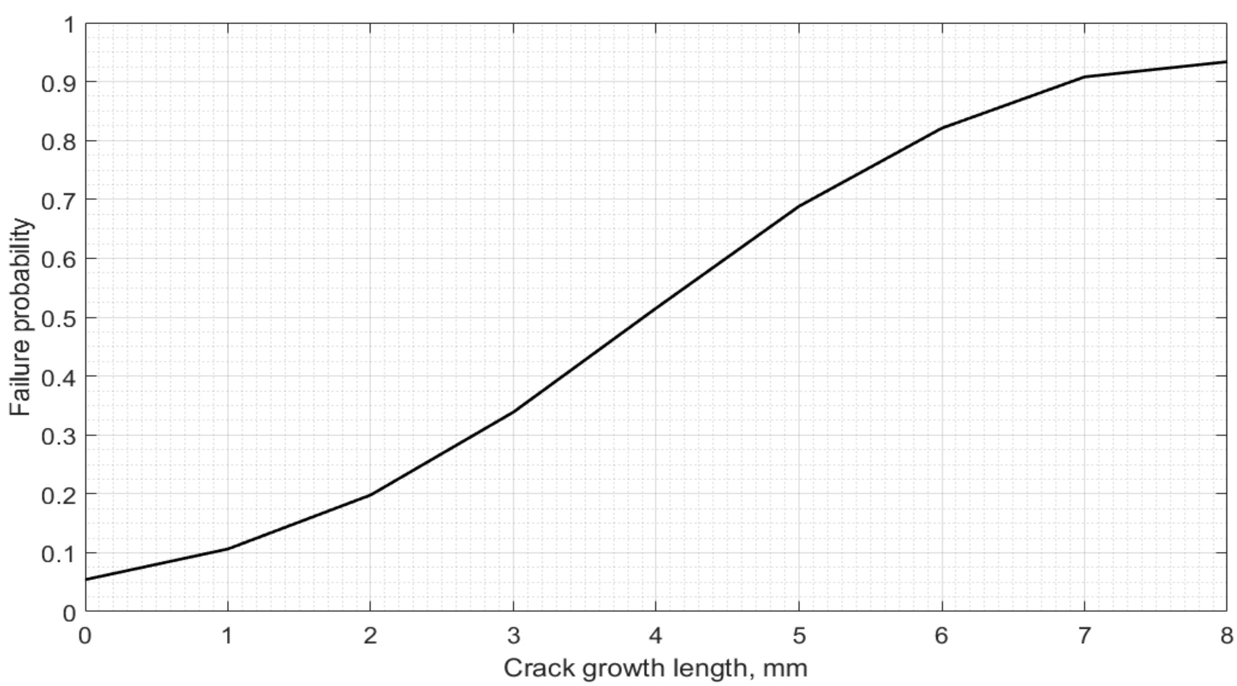

Fig. 9. Probability of rail failure based on the growth of crack length

In Fig. 10, a sample of 5 squats is visualized, and the estimates of failure probability from the given visual lengths are presented.

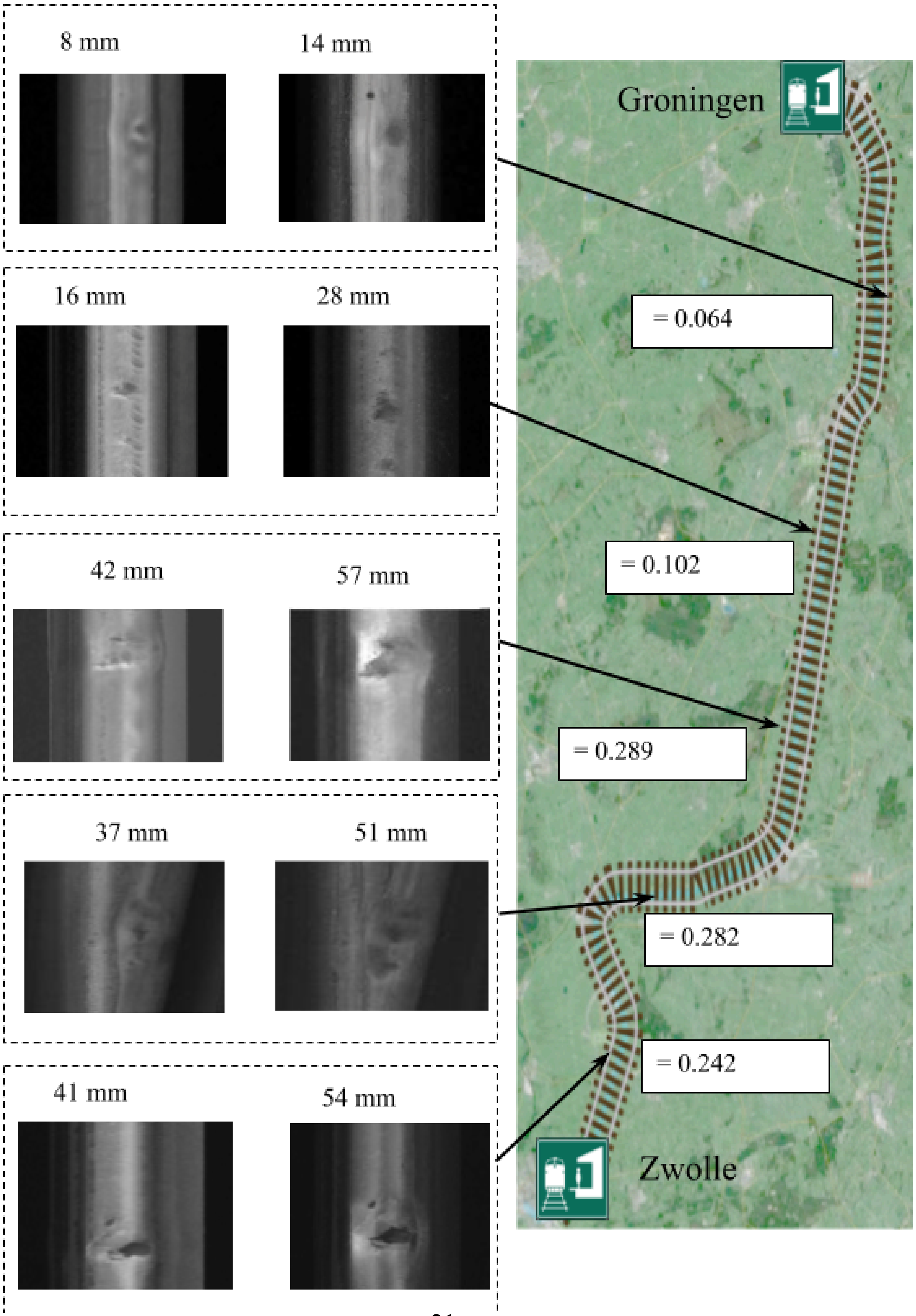

Fig. 10. A sample of failure risk estimates for 5 squats over the track

For instance, the squat with $V_1 = 42$ mm and $V_2 = 57$ mm will cause a rail break with a probability of 28.9% in next MGT step, if no maintenance action is operated. However, no serious failure threatens the squat at the early stage and the failure probability is then almost 10% (see the squat with 16 mm in visual length). In Table I, more samples of squats are presented.

Table I. Failure risk estimation for a sample of squats, detected on the track Zwelle-Groningen

Squat	V_1	V_2	ΔL	F_{Prob}	Squat	V_1	V_2	ΔL	F_{Prob}
1	3.65	4.56	0.02	0.055	33	16.41	21.87	0.48	0.079
2	8.20	9.11	0.03	0.056	34	10.03	14.58	0.42	0.076
3	3.65	5.47	0.05	0.057	35	6.38	19.14	0.46	0.078
4	7.29	9.11	0.05	0.057	36	8.20	21.87	0.48	0.079
5	3.65	6.38	0.08	0.058	37	17.32	23.70	0.55	0.083
6	5.47	8.20	0.09	0.059	38	7.29	20.96	0.49	0.080
7	6.38	9.11	0.09	0.059	39	6.38	20.96	0.53	0.082
8	4.56	8.20	0.10	0.060	40	9.11	27.34	0.63	0.087
9	5.47	9.11	0.11	0.060	41	11.85	18.23	0.60	0.085
10	2.73	7.29	0.13	0.061	42	8.20	30.08	0.78	0.095
11	3.65	8.20	0.13	0.061	43	14.58	23.70	0.77	0.094
12	4.56	9.11	0.14	0.061	44	28.25	31.90	0.95	0.104
13	2.73	8.20	0.15	0.062	45	11.85	21.87	0.90	0.101
14	5.47	10.03	0.15	0.062	46	10.03	20.96	0.94	0.103
15	6.38	11.85	0.17	0.063	47	14.58	30.08	1.17	0.122
16	7.29	12.76	0.19	0.064	48	30.99	37.37	1.55	0.156
17	3.65	10.03	0.19	0.064	49	13.67	30.99	1.31	0.134
18	4.56	10.94	0.19	0.064	50	12.76	29.16	1.29	0.133
19	5.47	11.85	0.21	0.065	51	10.03	24.61	1.20	0.125
20	8.20	14.58	0.21	0.065	52	20.05	24.61	1.48	0.151
21	10.03	12.76	0.25	0.067	53	13.67	34.63	1.48	0.151
22	2.73	10.94	0.24	0.067	54	24.61	31.90	1.91	0.190
23	6.38	13.67	0.24	0.067	55	31.90	41.92	2.23	0.231
24	7.29	14.58	0.24	0.067	56	10.94	40.10	1.95	0.194
25	6.38	14.58	0.27	0.068	57	22.78	30.99	2.35	0.248
26	3.65	12.76	0.27	0.068	58	24.61	34.63	2.56	0.277
27	9.11	18.23	0.29	0.069	59	27.34	38.28	2.62	0.286
28	2.73	13.67	0.34	0.072	60	39.19	55.59	3.05	0.348

29	6.38	16.41	0.34	0.072	61	23.70	35.54	3.09	0.355
30	8.20	19.14	0.38	0.074	62	33.72	52.86	3.69	0.461
31	17.32	22.78	0.46	0.078	63	28.25	46.48	3.87	0.493
32	8.20	20.96	0.44	0.077	64	30.99	51.04	4.10	0.532

The table includes 64 samples of squats with their measurements of visual length for two MGT steps. As expected, the squat at the severe stage will be prone to a rail break if no operation is carried out on the rail within a given MGT step. For example, there is a 53% chance of failure for the 64th squat in which the crack growth length is 4.10 mm within the given MGT step. The estimated risk values for the squats at the late stage indicate immediate rail replacements. For the squats at early stage, a grinding operation is suggested to postpone rail failure by treating squat.

CONCLUSIONS

In this paper, we present a methodology for the risk assessment of rail failure for a type of rail surface defects called squats. A big data analysis approach is used to automatically detect squats from rail images. The visual lengths of squats are measured in order to use them in the severity analysis model, which captures the growth of visual length over MGT increments. In addition, due to the influence of crack growth on estimation of the failure risk, a crack growth analysis based on MGT has been performed. At the end, a Bayesian model is employed to estimate the failure probability. By relying on the estimated failure risk, the infrastructure manager is able to take actions at the right time and the right place in order to prevent unexpected consequences induced by rail breaks. While this paper is focused on the analysis of squats, the results can also be applicable for the analysis of other type of rail defects.

ACKNOWLEDGEMENTS

This research is part of the NWO/ProRail project "Multi-party risk management and key performance indicator design at the whole system level (PYRAMIDS)", project code 438-12-300, and the STW/ProRail project "Advanced monitoring of intelligent rail infrastructure (ADMIRE)", project 12235, which are partly funded by the Ministry of Economic Affairs. The authors also would like to thank INSPECTATION for providing us with image data and technical support.

REFERENCES

1. Greenberg M, Lioy P, Ozbas B, Mantell N, Isukapalli S, Lahr M, Altiok T, Bober J, Lacy C, Lowrie K, Mayer H. Passenger rail security, planning, and resilience: application of network, plume, and economic simulation models as decision support tools. Risk analysis. 2013; 33(11):1969-1986.
2. Gandomi A, Haider M. Beyond the hype: Big data concepts, methods, and analytics. International Journal of Information Management. 2015; 35(2):137-144.
3. Sheppard JW, Kaufman M, Wilmer TJ. IEEE standards for prognostics and health management. Aerospace and Electronic Systems Magazine, 2009; 24(9):34-41.
4. Coraddu A, Oneto L, Ghio A, Savio S, Anguita D, Figari M. Machine learning approaches for improving condition-based maintenance of naval propulsion plants. Proceedings of the Institution of Mechanical Engineers, Part M: Journal of Engineering for the Maritime Environment. 2014; 230(1): 136-153.
5. Youree RK, Yalowitz JS, Corder A, Ooi TK. A multivariate statistical analysis technique for on-line fault prediction. International Conference on Prognostics and Health Management, 2008; CO, USA, 1-5.

6. Fumeo E, Oneto L, Anguita D. Condition based maintenance in railway transportation systems based on big data streaming analysis. Procedia Computer Science, 2015; 53:437-446.
7. Choi TM, Chan HK, Yue X. Recent development in big data analytics for business operations and risk management. IEEE Transactions on Cybernetics. 2016; 99:1-12.
8. Thekdi SA, Lambert JH. Decision analysis and risk models for land development affecting infrastructure systems. Risk analysis. 2012; 32(7):1253-1269.
9. Zhou Q, Lambert JH, Karvetski CW, Keisler JM, Linkov I. Flood protection diversification to reduce probabilities of extreme losses. Risk Analysis. 2012; 32(11):1873-1287.
10. Zoeteman A, Dollevoet RPB, Li Z. Dutch research results on wheel/rail interface management: 2001-2013 and beyond. Proceedings of the Institution of Mechanical Engineers, Part F: Journal of Rail and Rapid Transit. 2014; 228(6):642-651.
11. Burstow MC, Watson AS, Beagles M. Application of the whole life rail model to control rolling contact fatigue. Proceedings of the International Conference Railway Engineering, 2002; UK, London.
12. Li Z, Zhao X, Molodova M, Dollevoet RPB. Squat treatment by way of minimum action based on early detection to reduce life cycle costs. Proceedings of the Joint Rail Conference JRC, 2010; Urbana, Illinois.
13. Liu X, Barkan C, Saat M. Analysis of derailments by accident cause: evaluating railroad track upgrades to reduce transportation risk. Transportation Research Record: Journal of the Transportation Research Board. 2011; (2261):178-185.
14. Islam DM, Laparidou K, Burgess A. (in press). Cost effective future derailment mitigation techniques for rail freight traffic management in Europe. Transportation Research Part C: Emerging Technologies. 2015.
15. Liu X, Saat M, Barkan C. Analysis of causes of major train derailment and their effect on accident rates. Transportation Research Record: Journal of the Transportation Research Board. 2012; 15(2289):154-163.

16. Jafarian E, Rezvani MA. Application of fuzzy fault tree analysis for evaluation of railway safety risks: an evaluation of root causes for passenger train derailment. Proceedings of the Institution of Mechanical Engineers, Part F: Journal of Rail and Rapid Transit. 2012; 226(1):14-25.
17. Sandström J, Ekberg A. Predicting crack growth and risks of rail breaks due to wheel flat impacts in heavy haul operations. Proceedings of the Institution of Mechanical Engineers, Part F: Journal of Rail and Rapid Transit. 2009; 223(2):153-161.
18. Molodova M, Li Z, Núñez A, Dollevoet R. Automatic detection of squats in railway infrastructure. IEEE Transactions on Intelligent Transportation Systems. 2014; 15(5):1980-1990.
19. Fan Y, Dixon S, Edwards RS, Jian X. Ultrasonic surface wave propagation and interaction with surface defects on rail track head. NDT & E International. 2007; 40(6):471-477.
20. Song Z, Yamada T, Shitara H, Takemura Y. Detection of damage and crack in railhead by using eddy current testing. Journal of Electromagnetic Analysis and Applications. 2011; 3:546-550.
21. Mariani S, Nguyen T, Phillips RR, Kijanka P, di Scalea FL, Staszewski W, Fateh M, Carr G. Noncontact ultrasonic guided wave inspection of rails. Structural Health Monitoring. 2013; 12(5-6): 539-548.
22. Li Y, Trinh H, Haas N, Otto C, Pankanti S. Rail component detection, optimization, and assessment for automatic rail track inspection. IEEE Transactions on Intelligent Transportation Systems. 2014; 15(2):760-770.
23. Li Q, Ren S. A visual detection system for rail surface defects. IEEE Transactions on Applications and Reviews: Systems, Man, and Cybernetics, Part C. 2012; 42(6):1531-1542.
24. Li Q, Ren S. A real-time visual inspection system for discrete surface defects of rail heads. IEEE Transactions on Instrumentation and Measurement. 2012; 61(8):2189-2199.
25. Andrade AR, Teixeira PF. Statistical modelling of railway track geometry degradation using Hierarchical Bayesian models. Reliability Engineering & System Safety. 2015; 142:169-183.
26. Lam HF, Hu Q, Wong MT. The Bayesian methodology for the detection of railway ballast damage under a concrete sleeper. Engineering Structures. 2014; 81:289-301.

27. Mokhtarian P, Namzi-Rad MR, Ho TK, Suesse T. Bayesian nonparametric reliability analysis for a railway system at component level. IEEE International Conference on Intelligent Rail Transportation (ICIRT). 2013; Beijing, China.

28. Marsh W, Bearfield G. Using Bayesian networks to model accident causation in the UK railway industry. In Probabilistic Safety Assessment and Management. 2004; 3597-3602. Springer London.

29. Castillo E, Calviño A, Grande Z, Sánchez-Cambronero S, Gallego I, Rivas A, Menéndez JM. A Markovian–Bayesian Network for Risk Analysis of High Speed and Conventional Railway Lines Integrating Human Errors. Computer-Aided Civil and Infrastructure Engineering. 2015; 31(3): 193-218.

30. Ahn SE, Park CS, Kim HM. Hazard rate estimation of a mixture model with censored lifetimes. Stochastic Environmental Research and Risk Assessment. 2007; 21(6):711-716.

31. Li L, Wang J, Leung H, Jiang C. Assessment of catastrophic risk using Bayesian network constructed from domain knowledge and spatial data. Risk Analysis. 2010; 30(7):1157-1175.

32. Droguett EL, Mosleh A. Bayesian methodology for model uncertainty using model performance data. Risk Analysis. 2008; 28(5):1457-1476.

33. Kazemi R, Mosleh A. Improving default risk prediction using Bayesian model uncertainty techniques. Risk Analysis. 2012; 32(11):1888-1900.

34. Fan Y, Dixon S, Edwards RS, Jian X. Ultrasonic surface wave propagation and interaction with surface defects on rail track head. Ndt & E International. 2007; 40(6):471-477.

35. Krizhevsky A, Sutskever I, Hinton GE. Image net classification with deep convolutional neural networks. In Advances in neural information processing systems. 2012; 1097-1105.

36. LeCun Y, Bengio Y, Hinton G. Deep learning. Nature. 2015; 521(7553):436-444.

37. Sainath TN, Kingsbury B, Saon G, Soltau H, Mohamed AR, Dahl G, Ramabhadran B. Deep convolutional neural networks for large-scale speech tasks. Neural Networks. 2015; 64:39-48.

38. Srivastava N, Hinton G, Krizhevsky A, Sutskever I, Salakhutdinov R. Dropout: A simple way to prevent neural networks from overfitting. The Journal of Machine Learning Research. 2014; 15(1):1929-1958.
39. Bengio Y. Learning deep architectures for AI. Foundations and Trends in Machine Learning. 2009; 2(1):1-127.
40. Jamshidi A, Faghih-Roohi S, Núñez A, Babuska R, De Schutter B, Dollevoet R, Li Z. Probabilistic defect-based risk assessment approach for rail failures in railway infrastructure. Proceedings of the 14th IFAC Symposium on Control in Transportation Systems (CTS). 2016; Istanbul, Turkey.
41. Xu D, Zhao W. Reliability prediction using multivariate degradation data. Proceedings of the IEEE In Reliability and Maintainability Symposium. 2005; Alexandria, VA, USA.
42. Faghih-Roohi S, Xie M, Ng KM. Accident risk assessment in marine transportation via Markov modelling and Markov Chain Monte Carlo simulation. Ocean Engineering. 2014; 91:363-370.
43. Marques R, Bouville C, Ribardiere M, Santos LP, Bouatouch K. A spherical Gaussian framework for Bayesian Monte Carlo rendering of glossy surfaces. IEEE Transactions on Visualization and Computer Graphics. 2013; 19(10):1619-1632.
44. Gilks WR. Markov Chain Monte Carlo. John Wiley & Sons, Ltd; 2005.
45. Neal RM. Slice sampling. Annals of Statistics. 2003:705-741.
46. Li Z, Dollevoet R, Molodova M, Zhao X. Squat growth – Some observations and the validation of numerical predictions. Wear. 2011; 271(1-2):148–157.
47. Bassett Jr G, Koenker R. Asymptotic theory of least absolute error regression. Journal of the American Statistical Association. 1978; 73(363):618-622.